

Self-organization and Nonuniversal Anomalous Scaling in Non-Newtonian Turbulence

H. J. Seybold¹, H. A. Carmona², H. J. Herrmann^{2,3} and J. S. Andrade Jr.²

¹*Physics of Environmental Systems, D-USYS, ETH Zürich, 8093 Zürich, Switzerland*

²*Departamento de Física, Universidade Federal do Ceará, Campus do Pici, 60451-970 Fortaleza, Ceará, Brazil. and*

³*Computational Physics for Engineering Materials, D-BAUG, ETH Zürich, 8092 Zürich, Switzerland*

We investigate through Direct Numerical Simulations (DNS) the statistical properties of turbulent flows in the inertial subrange for non-Newtonian power-law fluids. The structural invariance found for the vortex size distribution is achieved through a self-organized mechanism at the microscopic scale of the turbulent motion that adjusts, according to the rheological properties of the fluid, the ratio between the viscous dissipations inside and outside the vortices. Moreover, the deviations from the K41 theory of the structure functions' exponents reveal that the anomalous scaling exhibits a systematic nonuniversal behavior with respect to the rheological properties of the fluids.

PACS numbers:

In many situations ranging from blood flow [1, 2] to atomization of slurries in industrial processing [3], one encounters non-Newtonian fluids in turbulent conditions. First experiments on turbulence in non-Newtonian fluids were already performed in 1959 [4]. Since then, most theoretical studies have focused on drag reduction [5, 6], and the mathematical modeling of wall stresses and boundary layers [7–9]. For isotropic turbulence in dilute polymer solutions, De Angelis *et al.* [10] found through DNS that relaxation connecting different scales significantly alters the energy cascade.

Intuitively, in the inertial subrange, molecular stresses should have a negligible influence on the motion and size of the eddies, regardless of the rheological nature of the fluid [11]. More precisely, even if a more complex constitutive law than a linear one is necessary to describe the stress-strain relation of a moving fluid, one should expect the statistical results obtained for the structure of Newtonian turbulence at the inertial subrange to remain valid. A relevant question that naturally arises is how the local rheological properties of the fluid must rearrange in space and time to comply with this alleged structural invariance. Here we provide an answer for this question by investigating through DNS the statistical properties of coherent structures of Newtonian and non-Newtonian turbulent flows in terms of distributions of eddy sizes and structure functions [12].

For our numerical analysis, we consider a cubic box containing a non-Newtonian fluid and subjected to periodic boundary conditions in all three directions. The mathematical formulation of the fluid mechanics is based on the assumptions that we have an incompressible fluid flowing under isothermal conditions, for which the momentum and mass conservation equations reduce to,

$$\frac{\partial \mathbf{u}}{\partial t} + \rho \mathbf{u} \cdot \nabla \mathbf{u} = -\nabla p + \nabla \cdot \mathbf{T} + \mathbf{\Gamma}, \quad (1)$$

and

$$\nabla \cdot \mathbf{u} = 0, \quad (2)$$

where \mathbf{u} and p are the velocity and pressure fields, respectively, $\mathbf{\Gamma}$ is a forcing term and \mathbf{T} is the deviatoric stress tensor given by,

$$\mathbf{T} = 2 \mu(\dot{\gamma}) \mathbf{E}. \quad (3)$$

Here $\mathbf{E} = (\nabla \mathbf{u} + \nabla \mathbf{u}^T)/2$ is the strain rate tensor and $\dot{\gamma} = \sqrt{2\mathbf{E} : \mathbf{E}}$ its second principal invariant. The function $\mu(\dot{\gamma})$ defines the constitutive relation, which for a cross-power-law fluid is given by

$$\mu(\dot{\gamma}) = K \dot{\gamma}^{(n-1)}, \quad \mu_1 \leq \mu \leq \mu_2. \quad (4)$$

The constants μ_1 and μ_2 are the lower and upper cutoffs, K is called the consistency index and n is the rheological exponent. Fluids with $n > 1$ are shear-thickening, while shear-thinning behavior corresponds to $n < 1$. For $n = 1$, we recover a Newtonian fluid. In this case, for reference, the Taylor Reynolds number is $Re_\lambda = 75$ [13].

A central assumption involved in the theoretical construct of the K41 theory [15–17] is that the fluid flow at a sufficiently large Reynolds is in a homogeneous and locally isotropic state, the so-called fully developed turbulence, that can be described in terms of universal statistical properties [12]. In order to attain a fully developed turbulent regime, here the fluid is driven by a linear force [18, 19],

$$\mathbf{\Gamma} = (\mathbf{u} - \langle \mathbf{u} \rangle) / \tau, \quad (5)$$

where $\langle \mathbf{u} \rangle$ is the spatial average of the velocity field and the parameter τ corresponds to a prescribed turnover time scale [19]. Differently from typical schemes, where low-wavenumber forcing is numerically applied in Fourier space, the linear forcing method is directly formulated in physical space and can therefore be readily integrated into physical-space numerical solvers [19].

For a given set of turbulent flow conditions and constitutive parameters of the non-Newtonian fluid, the numerical solution of Eqs. (1) and (2) for the time evolution of the local velocity and pressure fields is obtained through

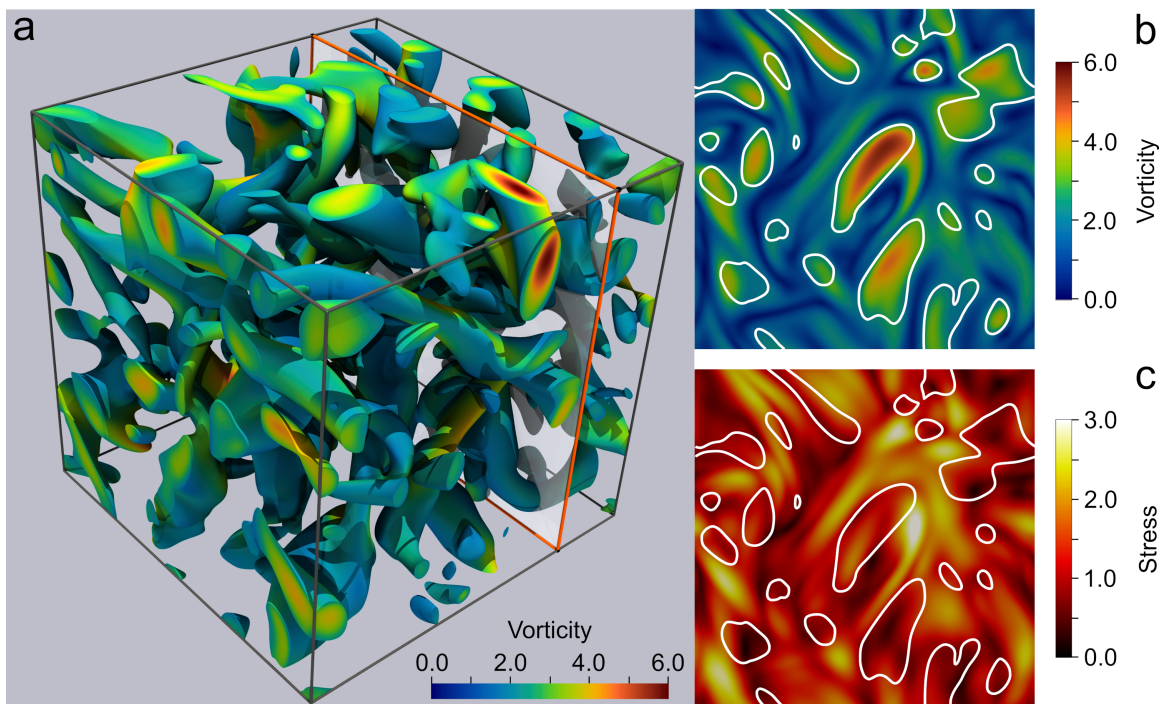


FIG. 1: Vortex identification using the λ_2 -vortex-criterion [14]. A typical snapshot of the vortex structure at the stationary state of the turbulent flow of a shear-thickening fluid with $n = 1.5$ is shown in panel (a). The iso-surfaces are calculated for a threshold value $\lambda_2^* = -10^{-5}$ and the colors correspond to the vorticity amplitude. The highlighted plane in panel (a) indicates the cross-section for the color maps in panels (b) and (c) for the vorticity amplitude and stress intensity, respectively. The white lines in panels (b) and (c) are the contours $\lambda_2 = \lambda_2^*$.

the open source DNS code *Gerris* [20]. This code is based on a second-order finite-volume scheme applied to an adaptively refined octree mesh. The maximal refinement level was set to eight subdivision steps, corresponding to a 256-cube discretization of our triple periodic box [21]. Finally, all simulations have been performed using an unstable Arnold-Beltrami-Childress (ABC) flow as initial configuration [22], which decays after a period of the order of τ to a stationary-state regime (see Fig. S3 from the Supplemental Material [33]).

At each time step, the geometric structure of turbulent eddies is characterized in terms of the λ_2 -vortex-criterion [14], which identifies vortices by the existence of a local pressure minimum, removing the effects of unsteady straining and viscosity. More precisely, the λ_2 -criterion delimits a vortex boundary based on the value of the second eigenvalue of the tensor, $\mathbf{M} = \mathbf{E}^2 + \mathbf{Q}^2$, where $\mathbf{Q} = (\nabla \mathbf{u} - \nabla \mathbf{u}^T)/2$. Since \mathbf{M} is symmetric, it has only real eigenvalues which can be ordered, $\lambda_1 < \lambda_2 < \lambda_3$. Accordingly, a vortex is defined as a connected region in space with at least two negative eigenvalues of \mathbf{M} , thus leading to the criterion [14] $\lambda_2 < 0$. In practical terms, considering a turbulent system with multiple vortices, we use this definition to identify them as clusters of cells in the numerical mesh of the cubic box for which $\lambda_2 \leq \lambda_2^*$, where $\lambda_2^* \leq 0$ is a given threshold value. The smaller the prescribed parameter λ_2^* , the smaller is the average volume which encloses the vortex cores in the

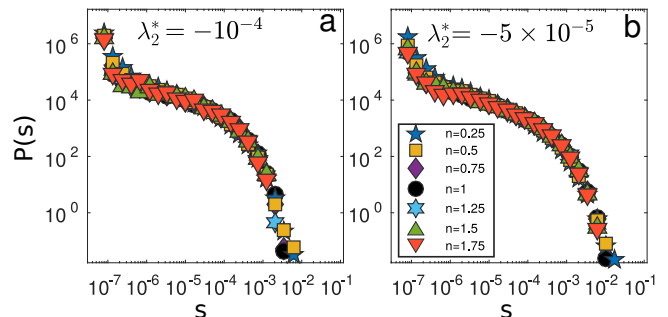


FIG. 2: Vortex size distributions computed for different values of the rheological exponent n , ranging from 0.25 to 1.75, and for three values of the threshold $\lambda_2^* = -10^{-4}$ (a), and -5×10^{-5} (b). As can be noticed, for a given fixed value of the threshold λ_2^* used to identify the vortex iso-surfaces, these distributions remain invariant with n (within numerical accuracy).

system. Figure 1a shows a typical snapshot of the vortex structure at the stationary state of the turbulent flow of a shear-thickening fluid with $n = 1.5$, and calculated for $\lambda_2^* = -10^{-5}$. The contours of λ_2^* (white lines) together with the color maps of the local vorticity and stress computed at the cross-section, as highlighted in Fig. 1a, are shown in Fig. 1b and 1c, respectively. These plots clearly confirm that the λ_2 -criterion captures both the intense

local vortical motion inside and the high stress outside the vortices.

Despite their chaotic and disordered nature, fully developed turbulent flows can be characterized in terms of certain statistical properties. Here, by identifying distinct vortices over a large number of snapshots of the system, the distribution of vortex sizes, $P(s)$, is computed for a given threshold λ_2^* , where s denotes the volume fraction of a vortex in the system. The results shown in Figs. 2 indicate that, for a fixed value of λ_2^* , the distribution remains invariant with n (within numerical accuracy), which ranges from power-law shear-thinning, $n = 0.25$, to shear-thickening behavior, $n = 1.75$. The fact that rheology has negligible impact on the statistical signature of this turbulent flow property gives support to the prediction that the structure of Newtonian turbulence at the inertial subrange is robust, meaning that the distribution of vortex sizes is not influenced by the details of the constitutive relation at the microscopic level [11].

At this point, we show how fluids possessing very distinct rheological features adapt to display the same vortex size distribution in the fully developed turbulent regime. Energy dissipation is a key fluctuating quantity in turbulent flows [23] and compared to a purely Newtonian fluid, the non-Newtonian constitutive relation Eq. (4) provides an additional degree of freedom which allows the system to dissipate energy in different ways. Using again the λ_2 -vortex-criterion [14] to distinguish regions in space that are inside and outside turbulent eddies, our results show that the energy dissipated per unit mass [24, 25], calculated for each cell of the numerical mesh as $\varepsilon = 2\mu(\dot{\gamma})\mathbf{E}^2$, is typically smaller inside the vortices than outside them, regardless of rheology. This general behavior is well exemplified by visualizing a snapshot of the turbulent flow calculated for a shear-thickening fluid, $n = 1.5$, as depicted in the color map of Fig. 3a. Figure 3b shows how the ratio $\varepsilon/\varepsilon_0$ changes with λ_2 for different values of n , where ε_0 is rate of energy dissipation for $n = 1$ at $\lambda_2 = 0$. Although all curves display the same qualitative pattern, namely, a slow decrease followed by a minimum at $\lambda_2 \approx 0$, and a comparatively rapid increase for positive values of λ_2 , the relative amounts of energy dissipated are strongly dependent on the rheological exponent n .

The global effect of rheology is better visualized when we calculate the ratio ϕ_n between the total energies dissipated outside and inside the vortices,

$$\phi_n = \left\langle \frac{\int_{\lambda_2^{\min}}^{\lambda_2^{\max}} \varepsilon(\lambda_2) d\lambda_2}{\int_{\lambda_2^{\min}}^{\lambda_2^{\max}} \varepsilon(\lambda_2) d\lambda_2} \right\rangle, \quad (6)$$

where λ_2^{\min} and λ_2^{\max} are the minimum and maximum values of λ_2 observed during the dynamics, respectively. The integrals are calculated over the entire simulation box, and the average is performed over several snapshots of the turbulent system. In Fig. 3c we show the dependence of the ratio ϕ_n/ϕ_1 on n for different values of the threshold λ_2^* . These results reveal that, relatively to

Newtonian fluids ($n = 1$), shear-thinning fluids ($n < 1$) adjust to have an augmented dissipation inside the vortices, $\phi_n < \phi_1$, while shear-thickening fluids ($n > 1$) show exactly the opposite behavior, $\phi_n > \phi_1$, namely, they dissipate relatively more outside the vortices. We can therefore argue that non-Newtonian fluids undergoing fully developed turbulence self-organize in distinctive dissipative regimes at the microscopic level so as to display vortex distributions that are statistically identical to that of Newtonian turbulence.

An insightful statistical measure to describe the scaling behavior of fluid turbulence over different spatial scales of the system is the longitudinal structure function [12, 26], $S_m^*(\mathbf{r}) = \langle [(\mathbf{u}(\mathbf{x} + \mathbf{r}) - \mathbf{u}(\mathbf{x})) \cdot \mathbf{r}/r]^m \rangle$, where $\mathbf{u}(\mathbf{x})$ is the velocity at position \mathbf{x} , \mathbf{r} is the separation vector, \mathbf{r}/r its direction unit vector, $r = |\mathbf{r}|$, and m is the order. This type of average measure has been extensively used for Newtonian fluids to quantify turbulence from experimental data as well as from numerical simulations across a given inertial-range scale r [27]. The so-called 4/5 law, which has been derived exactly by Kolmogorov [16] from the Navier-Stokes equations, determines the third-order structure function, $S_3^* = 4/5 \langle \varepsilon \rangle r$, where $\langle \varepsilon \rangle$ is the average rate of energy dissipation per unit mass. Although closed-form expressions for moments of other orders remain unknown, the seminal conceptual framework developed for the K41 theory [15, 16] led Kolmogorov to propose a generalized scaling relation for the structure functions, namely, $S_m^*(\mathbf{r}) \propto r^{\xi_m^*}$, with the scaling exponents given by $\xi_m^* = m/3$. The fact that the scaling exponents obtained from experiments as well as simulations for Newtonian fluids systematically deviate from this result is broadly accepted nowadays [27] and represents an open and important theoretical challenge in modern turbulence research [28].

In particular, when dealing with fractional and negative moments, it is convenient to use structure functions based on the absolute values of velocity differences rather than of velocity differences [27],

$$S_m(\mathbf{r}) = \langle |(\mathbf{u}(\mathbf{x} + \mathbf{r}) - \mathbf{u}(\mathbf{x})) \cdot \mathbf{r}/r|^m \rangle. \quad (7)$$

As in the case of S_m^* , it is known from numerical simulations [27] that these structure functions also obey a scaling relation of the form,

$$S_m(\mathbf{r}) \propto r^{\xi_m}, \quad (8)$$

although the exponents ξ_m and ξ_m^* may be slightly different [27]. Moreover, we opted to analyze our results using the Extended Self-Similarity method [29] (ESS), which is known [27] to exhibit larger scaling ranges for Newtonian turbulence than direct logarithmic plots of structure functions versus r . Precisely, the rationale behind the ESS [27] is to obtain the ratio of scaling exponents ξ_m/ξ_3 by plotting the corresponding structure function $S_m(\mathbf{r})$ against $S_3(\mathbf{r})$, assuming that $\xi_3 = \xi_3^* \equiv 1$. In order to extend this technique to non-Newtonian turbulence, we first confirm that all third-order structure functions

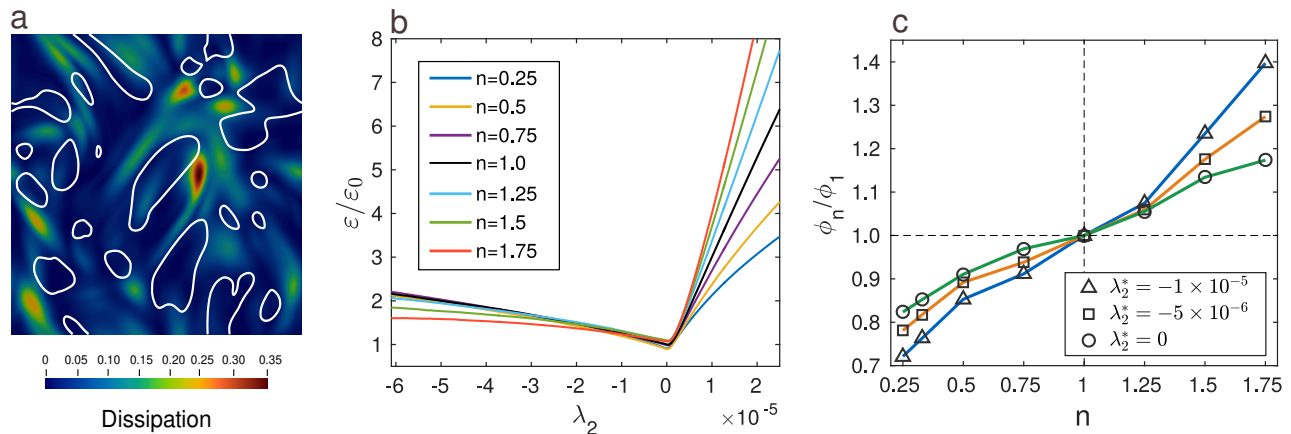


FIG. 3: a) Energy dissipation rate per unit of mass for the same snapshot and plane highlighted in Fig. 1a. The white lines correspond to iso-surfaces at the threshold value $\lambda_2^* = -10^{-5}$. On average there is more dissipation outside the connected regions with $\lambda_2 < \lambda_2^*$. b) Spatial and temporal average of the energy dissipation ratio ϵ/ϵ_0 as a function of λ_2 for different values of n , averaged over several eddy turnover times. c) The change of the ratio ϕ_n/ϕ_1 as a function of the rheology exponent n for different values of the threshold λ_2^* .

computed from our simulations, correlate linearly with the values of $S_3^1(\mathbf{r})$ for a Newtonian fluid, thus $S_3^n \sim S_3^1$ (see Fig. S1 from the Supplemental Material [33]), where the superscript n characterizes the rheology of the fluid. Considering this linear relation and following the ESS approach, the results of our simulations unequivocally show that the power-law relation, $S_m^n \sim S_3^{\xi_m^n}$, holds for turbulent flows of cross-power-law fluids over more than five orders of magnitude, notwithstanding the order m of the structure function as well as the rheological exponent n (examples are shown in Figs. S2 of the Supplemental Material [33] for $m = 0.5, 1.0$ and 2.0 , and $n = 0.5, 1.0$ and 1.5). Figure 4a shows the scaling exponents ξ_m obtained from our numerical simulations as a function of the order m for different rheological exponents n .

As already mentioned, it is indisputable from experimental data as well as from extensive numerical simulations that these deviations are indeed present in Newtonian turbulence [27, 30–32]. Moreover, taken as a limitation of the scaling result of the K41 theory, which is substantially more evident for higher order moments, the so-called anomalous scaling phenomenon has been often associated with the need for considering statistical conservation laws in the theoretical framework of hydrody-

namic turbulence [28]. Figure 4b shows the deviations of the structure function exponents from the K41 theory, $\delta_m^n = (\xi_m^n - m/3) / (m/3)$, as a function of m and for different rheological exponents n . Besides being compatible with the departure from the scaling exponents predicted by the K41 theory for the case of Newtonian turbulence, our results also reveal evidence for a nonuniversal behavior in the deviations of structure functions of non-Newtonian turbulence. More precisely, all deviations δ_m^n decrease monotonically with m , being practically zero for $m = 3$, positive for $m < 3$, and negative for $m > 3$. Our results also show that, for any fixed value of $m \neq 0$, the absolute values of δ_m^n increase systematically with the rheological exponent n .

In conclusion, we disclosed a self-organized mechanism of non-Newtonian turbulence through which the particular rheology of the fluid adjusts to comply with the statistical invariance found for the vortex size distribution. We also revealed a systematic dependence on the rheology of the anomalous scaling observed in the deviations from the K41 theory.

We thank the Brazilian agencies CNPq, CAPES, FUNCAP, and the National Institute of Science and Technology for Complex Systems for financial support.

[1] D. N. Ku, *Annu. Rev. Fluid Mech.* **29**, 399 (1997).
 [2] C. Vlachopoulos, M. O’Rourke, and W. W. N., *McDonald’s Blood Flow in Arteries: Theoretical, Experimental and Clinical Principles* (CRC Press, 2011), ISBN 0340985011.
 [3] R. W. Hanks and B. H. Dadia, *AIChE J.* **17**, 554 (1971).
 [4] D. W. Dodge and A. B. Metzner, *AIChE J.* **5**, 189 (1959).
 [5] D. Samanta, Y. Dubief, M. Holzner, C. Schäfer, A. N. Morozov, C. Wagner, and B. Hof, *Proceedings of the*

National Academy of Sciences **110**, 10557 (2013).
 [6] G. H. Choueiri, J. M. Lopez, and B. Hof, *Phys. Rev. Lett.* **120**, 124501 (2018), URL <https://link.aps.org/doi/10.1103/PhysRevLett.120.124501>.
 [7] A. Acrivos, M. J. Shah, and E. E. Petersen, *AIChE J.* **6**, 312 (1960).
 [8] G. Gioia and P. Chakraborty, *Proc. R. Soc. A* **473**, 20170354 (2017).
 [9] J. Singh, M. Rudman, and H. M. Blackburn, *J. Non-*

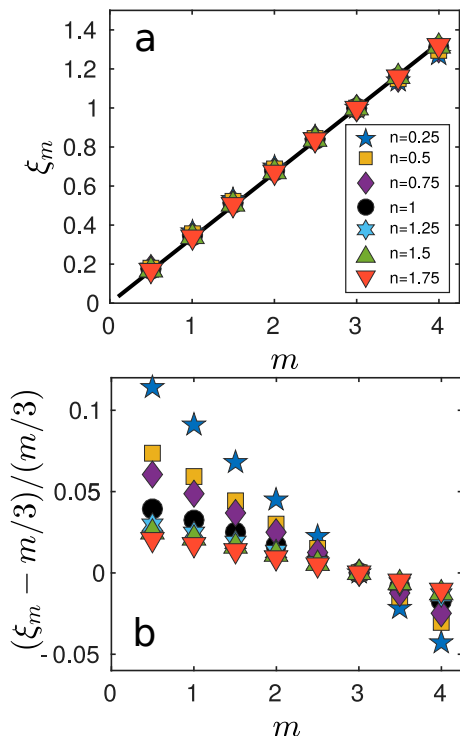


FIG. 4: a) Dependence of the scaling exponents ξ_m^n of the structure functions on their corresponding order m for different values of the rheological exponent n . The black solid line is the prediction of the K41 theory, $m/3$. b) Relative deviations of the exponents ξ_m^n from the K41 theory, $(\xi_m^n - m/3)/(m/3)$, as a function of the order m , calculated for different rheological exponents n .

Newtonian Fluid Mech. **249**, 53 (2017).

- [10] E. De Angelis, C. M. Casciola, R. Piva, J. Fluid Mech. **531**, 1 (2005).
 [11] A. A. Townsend, *The Structure of Turbulent Shear Flow* (Cambridge University Press, 1980), 2nd ed., ISBN 0521298199.
 [12] G. I. Taylor, Proc. R. Soc. London, A **151**, 421 (1935).
 [13] The Taylor Reynolds number is defined as $Re_\lambda = \langle v' \rangle_{\text{RMS}} \lambda / \mu$, where $\langle v' \rangle_{\text{RMS}}$ is the root mean square velocity, $\lambda = \sqrt{15\mu/\epsilon} \langle v' \rangle_{\text{RMS}}$ is the Taylor microscale, and

ϵ is the mean dissipation rate.

- [14] J. Jeong and F. Hussain, J. Fluid Mech. **285**, 69 (1995).
 [15] A. N. Kolmogorov, Dokl. Akad. Nauk SSSR **30**, 301 (1941).
 [16] A. N. Kolmogorov, Dokl. Akad. Nauk SSSR **32**, 16 (1941).
 [17] U. Frisch, *Turbulence: The Legacy of A. N. Kolmogorov* (Cambridge University Press, 1995), ISBN 0521457130.
 [18] T. S. Lundgren, Tech. Rep., University of Minnesota, Minneapolis (2003).
 [19] C. Rosales and C. Meneveau, Phys. Fluids **17**, 095106 (2005).
 [20] S. Popinet, J. Comput. Phys. **190**, 572 (2003).
 [21] The adaptively refined results obtained from the code *Gerris* are compared with a standard Newtonian spectral DNS code at the link: <http://gfs.sourceforge.net/examples/examples/forcedturbulence.html>.
 [22] T. Dombre, U. Frisch, J. M. Greene, M. Hénon, A. Mehr, and A. M. Soward, J. Fluid Mech. **167**, 353 (1986).
 [23] P. K. Yeung, X. M. Zhai, and K. R. Sreenivasan, Proceedings of the National Academy of Sciences **112**, 12633 (2015).
 [24] K. R. Sreenivasan, in *Symposium on Developments in Fluid Dynamics and Aerospace Engineering*, edited by S. M. Deshpande, A. Prah, K. R. Sreenivasan, and P. R. Viswanath (Interline Publishers, 1995), pp. 159–190.
 [25] A. S. Monin and A. M. Yaglom, *Statistical Fluid Mechanics, Volume II: Mechanics of Turbulence (Dover Books on Physics)* (Dover Publications, 2007), ISBN 0486458911.
 [26] J. Schumacher, J. D. Scheel, D. Krasnov, D. A. Donzis, V. Yakhot, and K. R. Sreenivasan, Proceedings of the National Academy of Sciences **111**, 10961 (2014).
 [27] S. Y. Chen, B. Dhruva, S. Kurien, K. R. Sreenivasan, and M. A. Taylor, J. Fluid Mech. **533**, 183 (2005).
 [28] G. Falkovich and K. R. Sreenivasan, Phys. Today **59**, 43 (2006).
 [29] R. Benzi, S. Ciliberto, R. Tripiccion, C. Baudet, F. Masaioli, and S. Succi, Phys. Rev. E **48**, R29 (1993).
 [30] C. Meneveau and K. R. Sreenivasan, Phys. Rev. Lett. **59**, 1424 (1987).
 [31] S. Kurien and K. R. Sreenivasan, Phys. Rev. E **64**, 056302 (2001).
 [32] V. Yakhot, Phys. Rev. E **63**, 026307 (2001).
 [33] See Supplemental Material at <http://link.aps.org/supplemental/???/???>